



Submitted: April 02, 2020 | Revised: May 14, 2020 | Accepted: July 26, 2020

Analyzing the Effect of Variation in Shielding Gas Flow Rate and V Groove Type Towards Tensile and Metallographic Testing of GMAW Weld Joint of ASTM A53 and A36

Herman Pratikno^{a,*}, Andrea Novia Samiyono^b and Wimala Lalitya Dhanistha^c

^{a)} Lecturer, Department of Ocean Engineering, Sepuluh Nopember Institute of Technology, Surabaya, Indonesia

^{b)} Undergraduate Student, Department of Ocean Engineering, Sepuluh Nopember Institute of Technology, Surabaya, Indonesia

^{c)} Lecturer, Department of Ocean Engineering, Sepuluh Nopember Institute of Technology, Surabaya, Indonesia

* Corresponding author: hermanp@oe.its.ac.id

ABSTRACT

Steel is a metal that commonly used in fabrication, engineering, and repair activities in the structure construction industry. ASTM A53 steel is a low carbon steel with 0.25% to 0.3% of carbon content so it has a high weldability. ASTM A36 steel is a low carbon steel with carbon content of 0.25% to 0.29% and is often used in the floating building industry. This study aims to determine the effect of shielding gas flow rate and V-groove type to the tensile strength of A53 steel welded with A36 steel by Gas Metal Arc Welding (GMAW) method. The shielding gas level used is 100% CO₂ with flow rate variations, including 15 liters/minute, 20 liters/minute, and 25 liters/minute. The groove types used are Single V-Groove and Double V-Groove. Tensile strength test result showed that in the welding process in this study, specimen with 25 liters/minute flow rate on the Double V-Groove had the highest tensile strength value of 516.73 MPa, with the narrowest HAZ width of 0,87 mm on A36's HAZ and 1,22 mm on A53's HAZ, and the smallest percentage of ferrite in the microstructure as much as 56.34% and 43.66% pearlite.

Keywords : A36 steel, A53 steel, gas metal arc welding, shielding gas flow rate, V-groove.

1. INTRODUCTION

The global competition makes Indonesia must be able to survive and continue to carry out development in all industrial sectors. As a maritime country, development continues to be carried out in accordance with its field such as construction of floating structure, offshore platform, pipe, fishery, or even the oil and gas industry that cannot be separated from offshore activities. In this case, welding has an important and broad role, as well as steel material, especially in the production and fabrication process [1]. Therefore, welding planning needs to consider the integration between the welding properties with the construction purposes and environmental condition, so that

it can be as economically effective and efficient as it can be [2].

Welding is a process of connecting metals or non-metals, by heating the materials until it reach the welding temperature which can be done by: with or without using pressure, only with pressure, or with or without using filler metal [3]. In its application, there are several methods including: GTAW or GMAW (Gas Metal Arc Welding), FCAW (Flux Cored Arc Welding), SMAW (Shield Metal Arc Welding), etc. In this study, the GMAW (Gas Metal Arc Welding) method is used. The reason behind that, GMAW is considered capable on providing several advantages, such as high welding speed, excellent removal of oxide films and the ability to weld in all positions [4].

Both ASTM A53 and ASTM A36 are low carbon steel commonly used in the maritime industry, due to its weldability. In the GMAW method, the composition of the shielding gas is said to be the most important thing in its function to protect the molten filler metal in the weld pool from atmospheric contamination [5]. Not only that, but the groove configuration is also very influential on the mechanical properties and microstructure of the welding structure [6].

Therefore, the study will discuss how the tensile strength of the weld joint with the GMAW method on ASTM A53 with ASTM A36. This research will analyze the effect of variation in the shielding gas flow rate and the V-Groove types to the welding joint of ASTM A53 steel plate and ASTM A36 steel.

2. MATERIALS AND METHODS

This section will discuss series of steps carried out in the whole process. First thing that needs to be done is to gather literatures to expand our understanding, also to minimize failures using both codes and other related papers. Then a

design or so-called Welding Procedure Specification (WPS) is made. The welding design needs to be discussed with the welder, only after that the materials could get prepared and executed according to settled WPS. After the welding procedure was completed, the specimens will undergo some preparations before testing the mechanical properties. The tests performed are tensile, bending, and metallographic test.

2.1 Gas Metal Arc Welding (GMAW)

Gas Metal Arc Welding (GMAW) is the process of connecting the metal by melting it with an electric arc produced between the electrode with the workpiece and using protective gas. This welding is carried out not only on ferrous materials but also on non-ferrous materials [7]. The shielding gas is used to maintain the arc flame and protect melted filler metal from atmospheric contamination [8]. Several factors that influence the welding result as follows: the shielding gas composition and flow rate, the type of electrode, groove configuration, feeding speed, voltage, current, etc. [9]. The basic system for GMAW is shown in Figure 1.

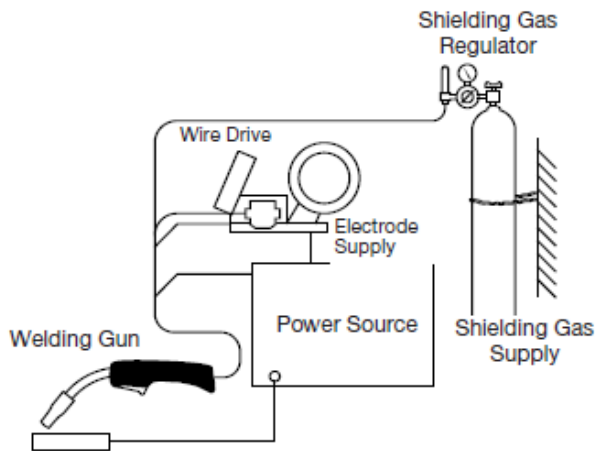


Figure 1. GMAW Basic System [10]

2.2 Shielding Gas

The protective gas, or often called as Shielding Gas, is used not only for protecting the molten filler metal, but also accelerating the cooling process [11]. The melting rate of the electrode and arc behaviour can also be influenced by this depending on each type [12]. The type and composition of the gas selected has a significant influence on the microstructure and mechanical properties of the joint. [13] [14] The flow rate used is generally around 15-20 liters/minute, but it can reach 36 liters/minute in special cases [15].

2.3 Welding Groove

The purpose of welding groove is to hold the filler metal so that more of it can be attached to the workpiece and the quality of the weld is guaranteed. The thicker the weld joint is the more acicular ferrite will be formed [16], which means

that the tenacity and toughness are also getting better. But there are things that must be considered in the configuration, such as the thickness of the workpiece, the type of workpiece, the desired strength, and the welding position.

2.4 Tensile Test

Tensile Test is a test to determine the maximum tensile strength (yield strength and ultimate strength) of welded material. This test is carried out by providing a continuous axial load until the material breaks. Material is considered elastic if it can return to its original form after being applied to loading conditions. Meanwhile, if the material can't return to its original form, it's considered to be plastic. The first property sought in a welded joint is that the tensile strength must be equal or close to the base metal [17].

2.5 Metallographic Test

Metallography is the study of the microstructure characteristic and its relationship to the property of metal and their alloy, which consists of macrostructure and microstructure test. Macrostructure test is a material testing process with naked eye to observe the morphology of the weld, including the measurement of the HAZ width and the presence of defects in the weld due to the deformation process, heat treatment process, and composition differences. The welding result can be seen properly as illustrated in Figure 2.

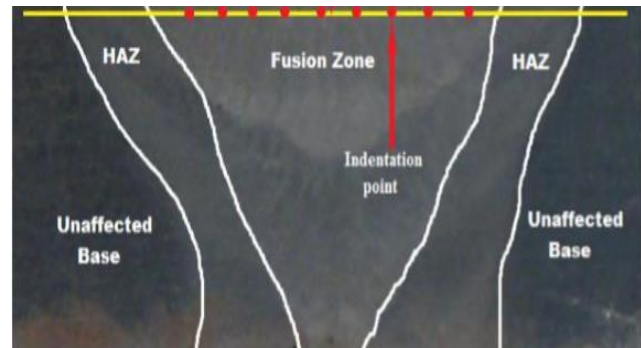


Figure 2. Illustration of Weld Area [18]

While micro testing is a test of the structure of material through a microscope and usually done to determine the shape and change in microstructure due to phase change. It should also be noted that in medium carbon steel welding metal, there are not only ferrite and pearlite grain, but widmanstatten ferrite, acicular ferrite, polygonal ferrite, and bainite, can also be found [19].

3. RESULT AND DISCUSSION

3.1 Welding Procedure

In this study, GMAW is carried out using the Welding Procedure Specification as follow:

- Material : ASTM A53 and ASTM

- Dimension : 200 mm x 150 mm x 18 mm
- Joint Type : Butt Joint Single V – Groove and Double V– Groove
- Welding Position : 1G
- AWS No. (Class) : AWS ER70S-6
- Filler Metal (Dia.) : Ø 1.2 mm
- Current : DCEP
- Number of Layer : 5 Layers
- Cleaning Method : Gridding
- Shielding Gas : 100% CO₂
- Gas Flow Rate : 15L/min, 20L/min and 25L/min
- Heat Treatment : N/A

The shielding gas flow rates used were 15 liters/minute, 20 liters/minute, and 25 liters/minute that carried out in both groove types with pure carbon dioxide (CO₂). The illustration of groove specifications can be seen in Figure 3 and Figure 4.

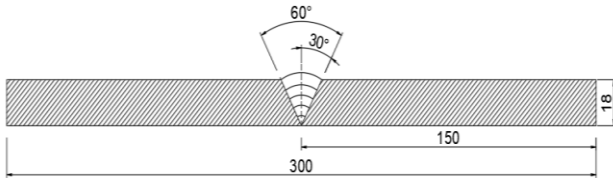


Figure 3. Single V– Groove Joint Specification

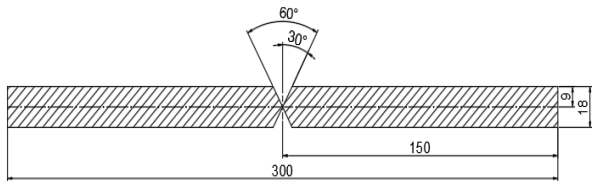


Figure 4. Double V– Groove Joint Specification

3.2 Tensile Test Result

The purpose of this test was to obtain the yield and ultimate tensile strength value of the specimen that have passed the radiographic test. This test was also used to determine the elastic and plastic limit of the weld joint. The standard used in this test was ASME Section IX, where the welding specimen was declared to have passed the tensile test if the ultimate strength of the weld metal exceeded the specified minimum tensile on the base metal itself and broke on the base metal. Each specimen was tested three times to get a valid result. In this study, using different materials, namely A53 and A36 steel. The minimum specified tensile material of A53 steel was smaller than A36 steel so that the breaking point should occur on the base metal of A53 steel.

For detail on the test result of the six test specimens can be seen in Table 1 and Table 2, with the visual result of the tested specimen in Figure 5, while for the test result's graph can be seen in Figure 6 and Figure 7.

Table 1. Single V-Groove Tensile Test Result

Specimen	Specimen Specs.			F Yield	F Ultimate	Result			Average	
	Width	Thickness	Area			Yield Strength	Ultimate Strength	Breaking	Yield Strength	Ultimate Strength
	(mm)	(mm)	(mm ²)			kN	kN	(MPa)	(MPa)	(MPa)
G1	19.3	17.9	345.47	134.5	166.44	389.32	481.78	Base Metal	389,99	481,82
G1-2	19.3	17.9	345.47	134.79	166.35	390.16	481.52	Base Metal		
G1-3	19.3	17.9	345.47	134.9	166.57	390.48	482.15	Base Metal		
G2	19.3	17.9	345.47	137.6	169.31	398.30	490.09	Base Metal	398,62	490,76
G2-2	19.3	17.9	345.47	137.75	169.52	398.73	490.69	Base Metal		
G2-3	19.3	17.9	345.47	137.78	169.8	398.82	491.50	Base Metal		
G3	19.3	17.9	345.47	138.78	172.2	401.71	498.45	Base Metal	401,95	499,18
G3-2	19.3	17.9	345.47	138.88	172.44	402.00	499.15	Base Metal		
G3-3	19.3	17.9	345.47	138.92	172.72	402.12	499.96	Base Metal		

Table 2. Double V-Groove Tensile Test Result

Specimen	Specimen Specs.			F Yield	F Ultimate	Result			Average	
	Width	Thickness	Area			Yield Strength	Ultimate Strength	Breaking	Yield Strength	Ultimate Strength
	(mm)	(mm)	(mm ²)			kN	kN	(MPa)	(MPa)	(MPa)
F1	19.3	17.9	345.47	140.54	173.82	406.81	503.14	Base Metal	407,07	503,23
F1-2	19.3	17.9	345.47	140.46	173.75	406.58	502.94	Base Metal		
F1-3	19.3	17.9	345.47	140.89	173.98	407.82	503.60	Base Metal		
F2	19.3	17.9	345.47	141.89	176.38	410.72	510.55	Base Metal	410,83	511,10
F2-2	19.3	17.9	345.47	141.92	176.52	410.80	510.96	Base Metal		
F2-3	19.3	17.9	345.47	141.98	176.81	410.98	511.80	Base Metal		
F3	19.3	17.9	345.47	142.56	178.52	412.66	516.75	Base Metal	412,80	516,73
F3-2	19.3	17.9	345.47	142.42	178.38	412.25	516.34	Base Metal		
F3-3	19.3	17.9	345.47	142.85	178.64	413.49	517.09	Base Metal		



Figure 5. Tensile Test Result

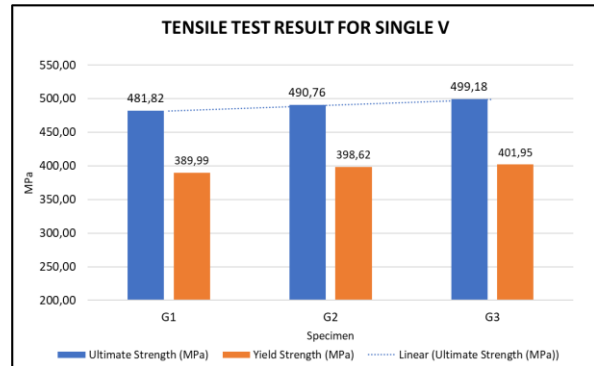


Figure 6. Graph of Tensile Test Result on Single V-Groove

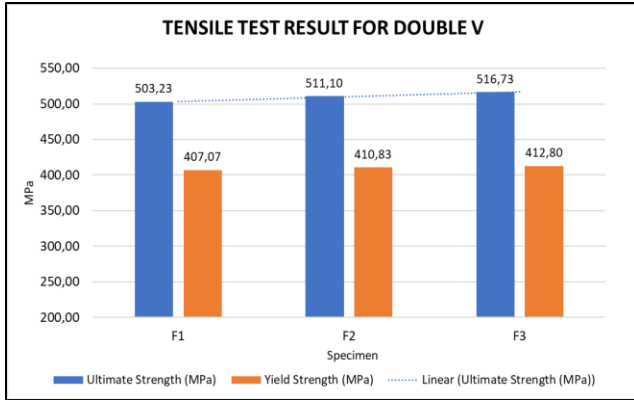


Figure 7. Graph of Tensile Test Result on Double V-Groove

The tensile test result on both groove types certified that all specimens passed the tensile test criteria in the ASME section IX standard. Also, it was found that the specimen with 25 liters/minute flow rate in Double V-Groove had the highest average tensile strength of 516.73 MPa. This was due to the high flow rate that stabilized the arc so that the electrode melted faster, this also accelerated the cooling process of the weld pool. On the other hand, the influence of the groove type showed that Double V-Groove accommodated fewer weld pool volume than Single V-Groove, so that the cooling process on Double V-Groove was relatively faster and provided greater tensile strength.

3.3 Metallographic Test Result

Metallographic tests consisted of macrostructure's and microstructure's photograph. Macrostructure testing was done by using a DSLR camera with 7x magnification to see the base metal, HAZ, and weld metal area. The purpose of the macrostructure test were to measure the width of the HAZ and to find any defect in the welded area. While the microstructure test was done by using a 100x magnification microscope to calculate the percentage of the dark (pearlite) and the white (ferrite) grains in the base metal, HAZ, and weld metal.

In the macrostructure result, it was found that the widest HAZ area was in the 1G specimen in Single V-Groove and 15 liters/minute flow rate, the width of the HAZ was 2,60 mm on A53's and 2,10 mm on A36's. Sequentially followed with specimen 2G, 3G, 1F, 2F, and 3F. This testified that 3F had the narrowest HAZ with 1,22 mm for A53's HAZ, and 0,87 mm for A36's HAZ. From these data, it can be concluded that the greater the flow rate, the narrower HAZ area formed. This could be caused by the high flow rate of shielding gas given during the welding process that accelerated the weld metal cooling process preventing the heat to spread. Besides, the width difference between A53's and A36's HAZ was due to carbon contained percentage, where A53 steel contained more carbon than A36 steel. The greater carbon content in a steel could reduce its weldability, and that lead to the heat input rate used in the welding

process, also widen the HAZ area. The HAZ width is summarized in Table 3, while the macro test result of the six specimens can be seen in Figure 8, and the comparison chart of the HAZ width can be seen in Figure 9.

Table 3. HAZ Width of Each Specimen

Specimen	Description	HAZ (mm)	
		A53	A36
1G	Single V ; 15L/mnt	2,60	2,10
2G	Single V ; 20L/mnt	2,10	1,70
3G	Single V ; 25L/mnt	1,83	1,52
1F	Double V ; 15L/mnt	1,67	1,33
2F	Double V ; 20L/mnt	1,33	1,17
3F	Double V ; 25L/mnt	1,22	0,87

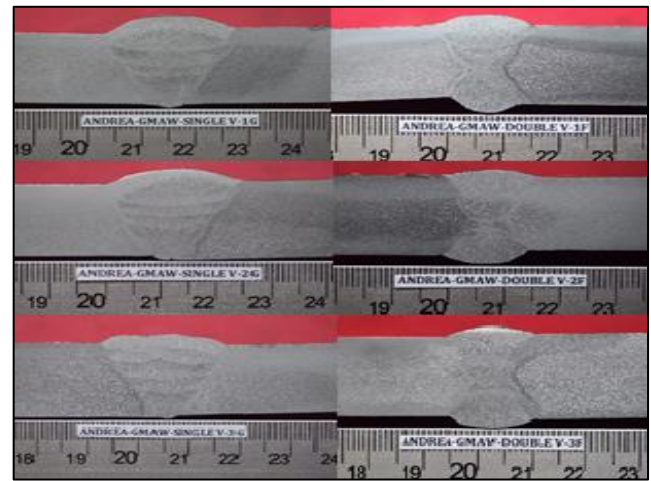


Figure 8. Macrostructure of six specimens

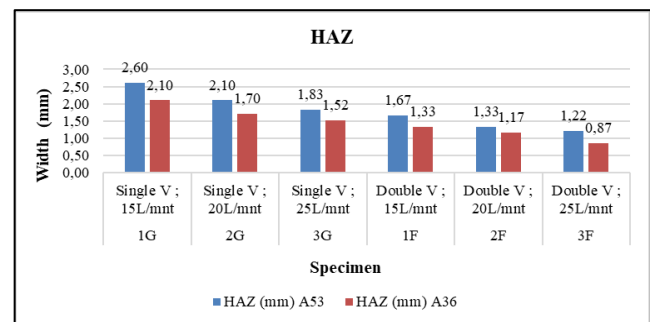


Figure 9. HAZ Width Area

In macrostructure test, clearly there was no discontinuity found in all specimens. While in microstructure test result, it can be found that the increase in the flow rate of the shielding gas is directly proportional to the decrease in the ferrite composition. This research also found that the minimum average percentage of ferrite was found in the same groove type with the highest flow rate as in the 3F specimen with Double V-Groove and 25 liters/minute flow rate had the lowest average ferrite structure percentage compared to 2F and 1F specimen, with the amount of 56.34% and 43.66% for pearlite. While based on the same

flow rate, the average percentage of ferrite in Figure 16 tend to be less in Double V-Grooved specimens. Thus, we could saw that the Double V-Groove had a more resilient weld joint, especially in the 3F specimen due to it had the least ferrite phase compared to other specimens. This caused by the large volume of filling metal filled in the groove, it was also known that the Single V-Groove required more filler metal than Double V-Groove, so that resulted in wider heat spread and longer cooling process. The result of microstructure test for all test specimens can be seen in Figure 10 to Figure 15.

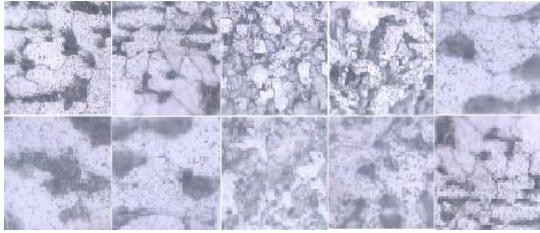


Figure 10. Microstructure Result of 1G Specimen

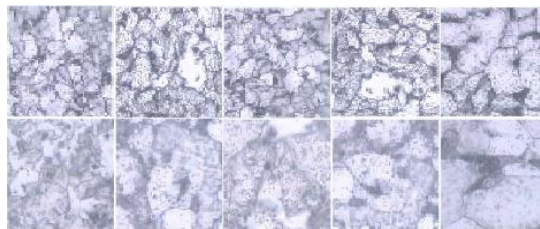


Figure 11. Microstructure Result of 2G Specimen

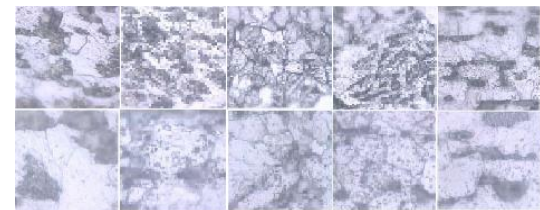


Figure 12. Microstructure Result of 3G Specimen

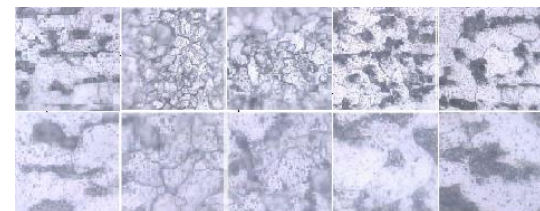


Figure 13. Microstructure Result of 1F Specimen

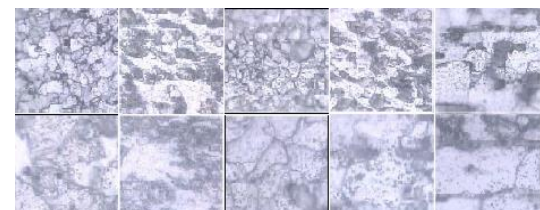


Figure 14 Microstructure Result of 2F Specimen

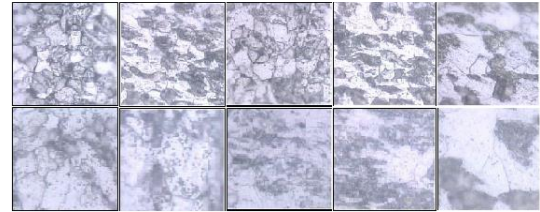


Figure 15. Microstructure Result of 3F Specimen

The result of microstructure test for all specimens can be seen in Table 4, and a comparison chart on ferrite and pearlite structure for all specimens can be seen in Figure 16.

Table 4. The Result of Microstructure Test

Specimen	Description	%									
		A53		HAZ A53		Weld Metal		HAZ A36		A36	
		Ferrite	Pearlite	Ferrite	Pearlite	Ferrite	Pearlite	Ferrite	Pearlite	Ferrite	Pearlite
1G	Single V ; 15L/mnt	68,7	31,3	57,4	42,6	66,7	33,3	58,9	41,1	70,2	29,8
2G	Single V ; 20L/mnt	66,3	33,7	55,8	44,2	62,2	37,8	56,7	43,3	68,9	31,1
3G	Single V ; 25L/mnt	63,7	36,3	53,6	46,4	61,1	38,9	54,4	45,6	65,8	34,2
1F	Double V ; 15L/mnt	65,5	34,5	56,7	43,3	62,3	37,7	55,1	44,9	66,8	33,2
2F	Double V ; 20L/mnt	63,2	36,8	52,3	47,7	61,1	38,9	53,3	46,7	65,6	34,4
3F	Double V ; 25L/mnt	61,4	38,6	51,5	48,5	54,4	45,6	52,2	47,8	62,2	37,8

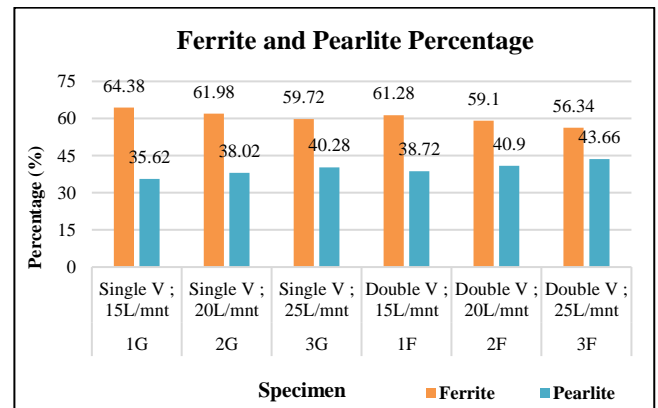


Figure 16. Graph of Average Ferrite and Pearlite

3.4 The Relationship between Tensile Test and Metallographic Test

From the tensile test and macro-micro observation that have been carried out, it was clear that the difference in groove type and the flow rates of the shielding gas used in welding greatly affect the welding result. As in Double V-Groove with 25 liters/minute flow rate, it shows that the material has the highest ultimate strength value compared with the specimens in the same groove type using lower shielding gas flow rate, namely specimen 2F and 1F, with ferrite phase which is directly proportional to the width of the HAZ and the percentage is increasing sequentially. Similarly, based on specimens with the same flow rate, the ultimate strength value obtained in Single V-Groove is lower compared to Double V-Groove. In the macro-microstructure test, it was known that the width of the HAZ area was much longer with higher ferrite structure formed in the Single V-Groove than in Double V-Groove. The larger ferrite structure formed caused material to broke more easily in tensile test.

Thus, in both tests, we know that the greater the shielding gas flow rate and the groove design during the welding process could affect the result of the material weld joint, where the greater shielding gas flow rate at the same groove type would increase its tensile strength. As in the test result, the material with higher flow rate on Double V-Groove had greater average ultimate strength, and as in the macro-microstructure result, the HAZ area formed was narrow and only a few ferrite structures was formed. The greater shielding gas flow rate would accelerate the cooling process and limit the spread of heat so that it narrowed the HAZ area, and could reduce the percentage of ferrite structure formed.

4. CONCLUSION

From the result of this research, the effect of variations in the shielding gas flow rate of 15 liters/minute, 20 liters/minute, and 25 liters/minute, as well as groove variations of the Single V-Groove and Double V-Groove using the GMAW process on joining the A53 steel material with A36 steel. Three points were elaborated as follows:

1. The tensile test result showed that the higher shielding gas flow rate applied, the better tensile strength obtained. The Double V-Groove specimen with 25 liters/minute flow rate had the best tensile strength, with average ultimate strength value of 516.73 MPa and yield strength of 412.80 MPa.
2. In macro-micro observation, higher shielding gas flow rate could result in narrower HAZ and less ferrite phase formed. Double V-Groove specimen with 25 liters/minute flow rate had the narrowest HAZ width of 1,22 mm on A53's HAZ and 0,87 mm on A36's HAZ with the lowest average ferrite phase of 56.34% and pearlite phase of 43.66%.
3. The higher the shielding gas flow rate used in joining the thin grooved materials, the tensile strength increased, while the HAZ width and ferrite phase decreased. This is due to the amount of flow rate applied could accelerate the cooling process and hinder the spread of heat, which closely related to the groove type design selection. The fewer the weld metal volume, the quicker for the joint connection to conduct the solidification process, and vice versa.

ACKNOWLEDGMENT

I am grateful to all those who have helped and provided support so that this research can be finished, namely Supervising Lecturers, Test Examiners at PPNS Welding Center, PT. Robutech, Laboratorium Uji Bahan PPNS, and Laboratorium Metalurgi Teknik Material Metalurgi ITS.

REFERENCES

1. Prasad, S.S., Mahesh, L., Rajendra, T., Rushikesh, P., and Farhan, P.: Analysis and optimization of structural

integrity of welded joint. *International Research Journal of Engineering and Technology*. 3(4): 1599-1604, 2017.

2. Wiryosumarto, H., and Okumura, T.: *Teknologi Pengelasan Logam*. PT. Pradnya Paramita, Jakarta, Indonesia, 2000.
3. Hilmy, Z., Syahroni N., and Hadiwidodo Y. S.: Analisa pengaruh variasi komposisi gas pelindung terhadap hasil pengelasan gmaw-short circuit dengan penggunaan mesin khusus regulated metal deposition (RMD). *The 2nd Conference on Innovation and Industrial Applications*. 1:219-226, 2018.
4. Lathabai, S.: Joining of aluminium and its alloys. *Fundamentals of Aluminium Metallurgy*. 1: 607-654, 2011.
5. Bird, J.: Improving the toughness of high strength GMA welds. *Marine Structures*. 6:461-474, 1993.
6. Çevik, B.: Analysis of welding groove configurations on strength of s275 structural steel welded by FCAW. *Journal of Polytechnic*. 21(2) : 489-495, 2018.
7. Praveen, P., Yarlagadda, P.K.D.V., and Kang, M.J.: Advancements in pulse gas metal arc welding. *Journal of Materials Processing Technology*. 164-165:1113-1119, 2005.
8. Monika, K., Chennaiah, M. B., Kumar, P. N., and Rao, K. P.: The effect of heat input on the mechanical properties of MIG welded dissimilar joints. *International Journal of Engineering Research & Technology*. 2: 1406-1413, 2013.
9. Sönmez U., and Ceyhun V.: Investigation of mechanical and microstructural properties of S 235 JR (ST 37-2) steels welded joints with FCAW. *Kovove Materialy-Metallic Materials*. 52: 57-63, 2014.
10. The Lincoln Electric Company.: *Gas Metal Arc Welding Product and Procedure Selection*. The Lincoln Electric Company, Ohio, United States of America 2015.
11. Schnick, M., Michael D., Jörg Z., Uwe F., and Andreas S.: Visualization and optimization of shielding gas flows in arc welding. *Welding in The World* . 56: 54-61, 2012
12. Zhao Y., Shi, X., Yan, K., Wang, G., Jia, Z., and He, Y. : Effect of shielding gas on the metal transfer and weld morphology in pulsed current MAG welding of carbon steel. *Journal of Materials Processing Technology*. 262:382-391, 2018.
13. Karadeniz E., Ozsarac, U., and Yildiz, C.: the effect of process parameters on penetration in gas metal arc welding processes. *Material and Design*. 28: 649-656, 2007.
14. Khaterasan, D., Sathiya, P., and Raja, A.: Shielding gas effect on flux cored arc welding of AISI 316L austenitic stainless steel joints. *Material and Design*. 45: 43-51, 2013.
15. Bitharas, I., McPherson, N. A., McGhie, W., Roy, D., and Moore, A. J.: Visualisation and optimisation of

- shielding gas coverage during gas metal arc welding. *Journal of Materials Processing Technology*. 255: 451–462, 2018.
16. Suprijanto, D.: Pengaruh bentuk kampuh terhadap kekuatan bending las sudut SMAW posisi mendatar pada baja karbon rendah. *Seminar Nasional ke8-Tahun 2013 : Rekayasa Teknologi Industri and Informasi*, Yogyakarta, Indonesia, Dec.14th, 2013
17. Kaya, Y., Kahraman, N., Durgutlu, A., and Gülenç, B.: Investigation of the mechanical properties of different thickness of the grade a ship plates joined by submerged arc welding. *e-Journal of New World Science Academy*. 5: 348-352, 2010.
18. Biswas, B.K., Pal, P.K., Bandyopadhyay, A.: Optimization of process parameters for flux cored arc welding of boiler quality steel using response surface methodology and grey based taguchi methods. *International Journal of Materials, Mechanic and Manufacturing*. 4(1):8-16, 2016.
19. Ling, K.H., Fuh, Y.K, Wu, K.L., Kuo, T.C., and Huang, C.Y.: Groove configurations of a flux-cored arc welding process used in critical structures of precision mechanical presses—mechanical and metallurgical studies. *The International Journal of Advanced Manufacturing Technology*. 78: 1905-1916, 2015.